The Canadian Mineralogist
Vol. 37, pp. 1471-1482 (1999)

THE EFFECT OF DIFFERENCES IN COORDINATION ON ORDERING OF POLYVALENT CATIONS IN CLOSE-PACKED STRUCTURES: THE CRYSTAL STRUCTURE OF ARAKIITE AND COMPARISON WITH HEMATOLITE

MARK A. COOPER AND FRANK C. HAWTHORNE§

Department of Geological Sciences, University of Manitoba, Winnipeg, Manitoba R3T 2N2, Canada

ABSTRACT

The crystal structure of arakiite, (Zn,Mn^{2+}) $(Mn^{2+},Mg)_{12}$ $(Fe^{3+},Al)_2$ $(As^{3+}O_3)$ $(As^{5+}O_4)_2$ $(OH)_{23}$, monoclinic, space group *Cc*, *a* 14.236(2), *b* 8.206(1), *c* 24.225(4) Å, β 93.52(1)°, *V* 2824.0(7) Å^3, *Z* = 4, has been solved by direct methods and has been refined to an *R* index of 5.6% based on 1825 observed (5σ) reflections measured with Mo*K*α radiation. There are eighteen crystallographically distinct cation sites, and the site occupancies were assigned using the refined site-scattering values, the observed stereochemistry, and the unit formula derived by electron-microprobe analysis. There are three *As* sites; *As*(1) and *As*(3) are occupied by As^{5+} in tetrahedral coordination, and *As*(2) is occupied by As^{3+} in triangular pyramidal coordination with a stereoactive lone-pair of electrons. There is one *T* site, *T*(1), occupied by Zn and Mn^{2+} in tetrahedral coordination. There are fourteen *M* sites, all of which are octahedrally coordinated. The *M*(4) site is occupied by Fe^{3+}, and the *M*(14) site is occupied by Al + Fe^{3+}; there are six *M* sites occupied exclusively by Mn^{2+}, one *M* site occupied by Mn^{2+} + Mg, and five *M* sites occupied by Mg + Mn^{2+}. Bond-valence analysis shows that all anions not linked to As^{3+} or As^{5+} are OH groups. Arakiite has a close-packed packet structure with five anion layers that stack along the *c*-axis in the sequence · ***hchΔ* · (* = displaced from closest packed). There are five distinct polyhedral layers along the *c* axis, with general compositions $[\square_7(T\phi_4)\phi_{10}]$, $[\square_3M_4(TO_4)\phi_{10}]$, $[\square_4M_3(TO_3)\phi_{10}]$, $[\square_6M_1(TO_4)\phi_9]$, and $[\square M_6\phi_{14}]$. Four of the layers are topologically identical to the corresponding layers in the structure of hematolite; the fifth layer differs between the two structures: arakiite: $[\square_7(T\phi_4)\phi_{10}]$; hematolite: $[\square_6M\phi_{14}]$. The two structures may be written chemically as follows:

arakiite: $^{[4]}(Zn,Mn^{2+})$ $^{[6]}(Mn^{2+},Mg)_{12}$ $^{[6]}(Fe^{3+},Al)_2$ $(As^{3+}O_3)$ $(As^{5+}O_4)_2$ $(OH)_{23}$
hematolite: $^{[6]}(Mn^{2+})$ $^{[6]}(Mn^{2+},Mg)_{12}$ $^{[6]}(Al,Fe^{3+})_2$ $(As^{3+}O_3)$ $(As^{5+}O_4)_2$ $(OH)_{23}$

Arakiite and hematolite show distinct ordering patterns of M^{2+} and M^{3+} cations in topologically identical close-packed layers. The observed ordering can be related to incident bond-strength requirements of the anions; differences in ordering between the two structures result from the different coordinations of cations ([4] in arakiite, [6] in hematolite) in the *m* = 0 sheet.

Keywords: arakiite, crystal structure, arsenate, arsenite, hematolite, Långban, Sweden.

SOMMAIRE

Nous avons affiné la structure cristalline de l'arakiite, (Zn,Mn^{2+}) $(Mn^{2+},Mg)_{12}$ $(Fe^{3+},Al)_2$ $(As^{3+}O_3)$ $(As^{5+}O_4)_2$ $(OH)_{23}$, monoclinique, groupe spatial *Cc*, *a* 14.236(2), *b* 8.206(1), *c* 24.225(4) Å, β 93.52(1)°, *V* 2824.0(7) Å^3, *Z* = 4, par méthodes directes jusqu'à un résidu *R* de 5.6% en utilisant 1825 réflexions observées (5σ) mesurées avec rayonnement Mo*K*α. La structure contient dix-huit sites cationiques distincts, et la population des atomes sur ces sites a été déterminée par affinement du pouvoir de dispersion associé à chaque site, la stéréochimie du minéral, et l'unité formulaire, telle que dérivée par analyse à la microsonde électronique. La structure contient trois sites *As* distincts; *As*(1) et *As*(3) contiennent l'ion As^{5+} en coordinence tétraédrique, et *As*(2) contient l'ion As^{3+} en coordinence triangulaire pyramidale, avec une paire isolée d'électrons stéréoactifs. Il y a un site *T*, *T*(1), qu'occupent Zn et Mn^{2+} en coordinence tétraédrique. Tous les quatorze sites *M* possèdent une coordinence octaédrique. Le site *M*(4) contient Fe^{3+}, et le site *M*(14) contient Al + Fe^{3+}; six des sites *M* contiennent exclusivement l'ion Mn^{2+}, un site *M* contient Mn^{2+} + Mg, et cinq sites *M* contiennent Mg + Mn^{2+}. Une analyse des valences de liaisons démontre que tous les anions non liés à As^{3+} ou As^{5+} sont des groupes OH. L'arakiite possède une structure en paquets à empilement compact de cinq couches le long de l'axe *c* dans la séquence · ***hch* · (* = déplacements observés par rapport à l'empilement compact). Nous reconnaissons cinq couches de polyèdres le long de l'axe *c*, dont les compositions généralisées seraient $[\square_7(T\phi_4)\phi_{10}]$, $[\square_3M_4(TO_4)\phi_{10}]$, $[\square_4M_3(TO_3)\phi_{10}]$, $[\square_6M_1(TO_4)\phi_9]$, et $[\square M_6\phi_{14}]$. Quatre de ces couches sont topologiquement identiques à celles de la structure de l'hématolite; La cinquième couche distingue les deux structures: arakiite: $[\square_7(T\phi_4)\phi_{10}]$; hématolite: $[\square_6M\phi_{14}]$. On peut exprimer la composition de ces deux minéraux comme suit:

arakiite: $^{[4]}(Zn,Mn^{2+})$ $^{[6]}(Mn^{2+},Mg)_{12}$ $^{[6]}(Fe^{3+},Al)_2$ $(As^{3+}O_3)$ $(As^{5+}O_4)_2$ $(OH)_{23}$
hématolite: $^{[6]}(Mn^{2+})$ $^{[6]}(Mn^{2+},Mg)_{12}$ $^{[6]}(Al,Fe^{3+})_2$ $(As^{3+}O_3)$ $(As^{5+}O_4)_2$ $(OH)_{23}$

§ *E-mail address*: frank_hawthorne@umanitoba.ca

Ces deux minéraux font preuve de schémas distincts de mise en ordre des cations M^{2+} et M^{3+} dans des couches à empilement compact identiques du point de vue topologique. Le schéma observé de mise en ordre résulterait des exigeances dans la force des liaisons incidentes des anions; les différences entre les deux structures découlent de la différence en coordinence des cations ([4] dans l'arakiite, [6] dans l'hématolite) dans le feuillet $m = 0$.

(Traduit par la Rédaction)

Mots-clés: arakiite, structure cristalline, arsenate, arsenite, hématolite, Långban, Suède.

Introduction

Arakiite, a Zn-, Mn^{2+}- and Fe^{3+}-bearing hydroxylated arsenate-arsenite, was described as a new mineral by Roberts *et al.* (2000). It strongly resembles hematolite and dixenite, but was distinguished from these two minerals by its unique X-ray powder-diffraction pattern. Arakiite was recognized as a new mineral almost 15 years ago, but its formal description (Roberts *et al.* 2000) had to await the discovery of crystals of sufficient quality to allow solution of the crystal structure and identification of its unique crystal-chemical features. The results of the crystal-structure analysis are presented here.

Experimental

The crystals used in this work are from the type locality and were obtained from Dr. Mark Feinglos. A small slightly bent cleavage fragment was attached to a glass fiber and mounted on a Siemens *P*4 automated four-circle diffractometer equipped with Mo$K\alpha$ radiation. Forty-one reflections over the range $10 \le 2\theta \le 27°$ were centered, and the unit-cell dimensions (Table 1) were refined by the least-squares method from the resultant setting angles. Intensity data were collected in θ–2θ scan-mode at a fixed scan-rate of 1.0°2θ/min. A total of 2765 reflections was measured over the range $4 \le 2\theta \le 45°$, with index ranges $\bar{15} \le h \le 15$, $\bar{2} \le k \le 8$, $\bar{2} \le l \le 26$. Two standard reflections were monitored every fifty-eight reflections; there were no significant changes in their intensities during data collection. The data were corrected for absorption by Gaussian quadrature integration, Lorentz, polarization and background effects, averaged and reduced to structure factors; of the 2080 unique reflections, 1825 reflections were considered as observed [$|F_o| \ge 5\sigma F_o$].

TABLE 1. MISCELLANEOUS INFORMATION FOR ARAKIITE

a (Å)	14.236(2)	Crystal size (mm)	0.01 x 0.15 x 0.15
b	8.206(1)	Radiation	Mo$K\alpha$/Graphite
c	24.225(4)	Total no. of I	2765
β (°)	93.52(1)	No. of $\|F\|$	2080
V(Å^3)	2824.0(7)	No. of $\|F_o\| > 5\sigma$	1825
Sp. Gr.	*Cc*	*R*(merge) %	4.3
Z	4	*R*(obs) %	5.6
		wR(obs)%	6.4

unit cell contents:
$(Zn_{0.71}\ Mn^{2+}_{0.29})\ (Mn^{2+}_{7.77}\ Mg_{4.23})\ (Fe^{3+}_{1.26}\ Al_{0.74})\ (As^{3+}O_3)\ (As^{5+}O_4)_2\ (OH)_{23}$

$R = \Sigma(|F_o|-|F_c|)/\Sigma|F_o|$

$wR = [\Sigma w(|F_o|-|F_c|)^2/\Sigma F_o^2]^{1/2}$, $w = 1$

Structure Solution and Refinement

Scattering curves for neutral atoms were taken from Ibers & Hamilton (1974). *R* indices are of the form given in Table 1, and are expressed as percentages. The Siemens SHELXTL PLUS (PC version) system of programs was used for this work.

The structure was solved by direct methods and difference-Fourier synthesis. With all non-H-atom positions located, the structure refined to an *R* index of ~6% for an isotropic-displacement model. Site-scattering indicates that the *As* sites are completely occupied by As, and that the *M*(1), *M*(2), *M*(3), *M*(5), *M*(6) and *M*(7) sites are occupied by Mn; in addition, the *M*(4) site is occupied by Fe (as indicated by the site-scattering and the mean bond-length). The occupancies of these sites were fixed at 1.0 in subsequent cycles of refinement. The constituents of the remaining sites were assigned from the site-scattering values, the mean bond-lengths and the unit formula derived from the results of electron-microprobe analysis; the site occupancies were considered as variable in subsequent cycles of refinement. Positional and displacement parameters for the constrained refinement are given in Table 2, selected interatomic distances in Table 3, and refined site-occupancy parameters in Table 4. Observed and calculated structure-factors are available from The Depository of Unpublished Data, CISTI, National Research Council, Ottawa, Ontario K1A 0S2, Canada.

Electron-Microprobe Analysis

Arakiite was analyzed with a Cameca SX–50 electron microprobe operating in wavelength-dispersion mode with an accelerating voltage of 15 kV, a specimen current of 20 nA, a beam size of 5 μm and counting times on peak and background of 20 and 10 s, respectively. The following standards were used: cobaltite (As), gahnite (Zn), spessartine (Mn), forsterite (Mg), fayalite (Fe) and kyanite (Al). Data were reduced using the $\phi(\rho z)$ procedure of Pouchou & Pichoir (1985). The chemical composition of the fragment that was used for electron-microprobe analysis is given in Table 5 and is

the mean of thirteen determinations. The unit formula was calculated on the basis of 34 anions.

Coordination of the Cations

There are eighteen crystallographically distinct cation sites in the structure of arakiite (Table 2). The

TABLE 2. ATOMIC POSITIONS AND ISOTROPIC DISPLACEMENT FACTORS* FOR ARAKIITE

Site	*x*	*y*	*z*	U_{iso}
T(1)	0	0.2434(4)	0	85(15)
M(1)	0.9137(4)	0.3711(5)	0.1297(2)	118(10)
M(2)	0.6836(4)	0.3897(6)	0.1281(3)	130(11)
M(3)	0.7871(4)	0.0312(5)	0.1292(2)	119(10)
M(4)	0.1305(3)	0.2662(5)	0.1285(2)	88(9)
M(5)	0.9895(4)	0.0026(5)	0.2297(2)	91(9)
M(6)	0.3438(4)	0.1696(5)	0.2306(2)	99(10)
M(7)	0.5830(4)	0.1177(5)	0.2298(2)	103(10)
M(8)	0.4816(4)	0.2613(6)	0.3404(3)	102(18)
M(9)	0.8486(6)	0.4737(11)	0.4292(4)	125(35)
M(10)	0.9217(6)	0.1147(11)	0.4294(4)	133(34)
M(11)	0.0607(5)	0.4054(8)	0.4311(3)	79(26)
M(12)	0.2802(5)	0.3292(8)	0.4316(3)	88(27)
M(13)	0.1305(5)	0.0383(9)	0.4278(4)	73(32)
M(14)	0.7047(5)	0.1859(8)	0.4307(3)	95(24)
As(1)	0.1464(3)	0.2624(4)	0.3084(2)	77(6)
As(2)	0.8051(3)	0.2639(4)	0.2282(2)	94(7)
As(3)	0.4595(3)	0.2639(3)	0.1091(2)	75(7)
O(1)	0.887(1)	0.156(2)	0.1893(8)	125(43)
O(2)	0.705(1)	0.190(2)	0.1884(8)	116(43)
O(3)	0.812(1)	0.444(2)	0.1889(9)	156(48)
O(4)	0.035(1)	0.216(2)	0.2866(9)	171(47)
O(5)	0.173(1)	0.453(2)	0.2865(9)	162(47)
O(6)	0.225(1)	0.126(2)	0.2854(9)	147(45)
O(7)	0.154(1)	0.259(2)	0.3803(8)	95(44)
O(8)	0.408(1)	0.092(2)	0.0848(9)	152(46)
O(9)	0.569(1)	0.277(2)	0.0863(8)	145(44)
O(10)	0.466(1)	0.261(2)	0.1791(9)	124(42)
O(11)	0.395(1)	0.426(2)	0.0853(9)	150(45)
OH(1)	0.009(1)	0.219(2)	0.0823(8)	66(39)
OH(2)	0.626(1)	0.318(2)	0.4772(8)	107(43)
OH(3)	0.397(1)	0.415(2)	0.4792(8)	123(45)
OH(4)	0.466(1)	0.029(2)	0.4803(9)	163(47)
OH(5)	0.107(1)	0.065(2)	0.1778(9)	115(44)
OH(6)	0.048(1)	0.396(2)	0.1783(9)	154(46)
OH(7)	0.245(1)	0.322(2)	0.1788(9)	110(42)
OH(8)	0.158(1)	0.457(2)	0.0829(9)	115(43)
OH(9)	0.204(1)	0.112(2)	0.0821(9)	127(44)
OH(10)	0.723(1)	0.385(2)	0.3881(9)	145(45)
OH(11)	0.790(1)	0.054(2)	0.3890(9)	144(45)
OH(12)	0.594(1)	0.116(2)	0.3836(9)	133(45)
OH(13)	0.821(1)	0.255(2)	0.4722(8)	143(47)
OH(14)	0.186(1)	0.486(2)	0.4726(9)	122(44)
OH(15)	0.362(1)	0.181(2)	0.3827(9)	128(45)
OH(16)	0.938(1)	0.330(2)	0.3882(8)	79(42)
OH(17)	0.256(1)	0.111(2)	0.4714(9)	173(47)
OH(18)	0.044(1)	0.184(2)	0.4714(8)	93(42)
OH(19)	0.508(1)	0.490(2)	0.3798(9)	136(45)
OH(20)	0.462(1)	0.070(2)	0.2781(9)	129(45)
OH(21)	0.386(1)	0.382(2)	0.2778(9)	118(43)
OH(22)	0.583(1)	0.337(2)	0.2773(9)	150(47)
OH(23)	0.793(1)	0.262(2)	0.0860(8)	95(43)

* $U \times 10^4$

TABLE 3. SELECTED INTERATOMIC DISTANCES (Å) FOR ARAKIITE

T(1)–OH(1)	2.00	*As*(2)–O(1)	1.78
T(1)–OH(2)e	1.97	*As*(2)–O(2)	1.78
T(1)–OH(3)e	2.00	*As*(2)–O(3)	1.76
T(1)–OH(4)e	1.98	<*As*(2)–O>	1.77
<*T*(1)–O>	1.99		
As(1)–O(4)	1.68	*As*(3)–O(8)	1.69
As(1)–O(5)	1.70	*As*(3)–O(9)	1.69
As(1)–O(6)	1.70	*As*(3)–O(10)	1.69
As(1)–O(7)	1.74	*As*(3)–O(11)	1.70
<*As*(1)–O>	1.71	<*As*(3)–O>	1.69
M(1)–O(1)	2.32	*M*(8)–OH(12)	2.21
M(1)–O(3)	2.19	*M*(8)–OH(15)	2.15
M(1)–O(8)d	2.11	*M*(8)–OH(19)	2.13
M(1)–OH(1)b	2.22	*M*(8)–OH(20)	2.19
M(1)–OH(6)b	2.19	*M*(8)–OH(21)	2.21
M(1)–OH(23)	2.15	*M*(8)–OH(22)	2.25
<*M*(1)–O>	2.20	<*M*(8)–O>	2.19
M(2)–O(2)	2.21	*M*(9)–OH(4)d	2.07
M(2)–O(3)	2.31	*M*(9)–OH(10)	2.12
M(2)–O(9)	2.08	*M*(9)–OH(13)	2.13
M(2)–OH(5)d	2.20	*M*(9)–OH(15)d	2.06
M(2)–OH(9)d	2.17	*M*(9)–OH(16)	2.04
M(2)–OH(23)	2.19	*M*(9)–OH(17)d	2.06
<*M*(2)–O>	2.19	<*M*(9)–O>	2.08
M(3)–O(1)	2.22	*M*(10)–OH(3)c	2.08
M(3)–O(2)	2.31	*M*(10)–OH(11)	2.12
M(3)–O(11)c	2.11	*M*(10)–OH(13)	2.16
M(3)–OH(7)c	2.20	*M*(10)–OH(16)	2.05
M(3)–OH(8)c	2.18	*M*(10)–OH(18)b	2.04
M(3)–OH(23)	2.17	*M*(10)–OH(19)c	2.05
<*M*(3)–O>	2.20	<*M*(10)–O>	2.08
M(4)–OH(1)	2.03	*M*(11)–O(7)	2.22
M(4)–OH(5)	2.08	*M*(11)–OH(4)f	2.11
M(4)–OH(6)	2.04	*M*(11)–OH(12)f	2.14
M(4)–OH(7)	2.03	*M*(11)–OH(14)	2.10
M(4)–OH(8)	1.97	*M*(11)–OH(16)g	2.08
M(4)–OH(9)	2.03	*M*(11)–OH(18)	2.09
<*M*(4)–O>	2.03	<*M*(11)–O>	2.12
M(5)–O(1)	2.12	*M*(12)–O(7)	2.19
M(5)–O(4)b	2.30	*M*(12)–OH(3)	2.08
M(5)–O(10)c	2.34	*M*(12)–OH(11)f	2.12
M(5)–OH(5)b	2.22	*M*(12)–OH(14)	2.14
M(5)–OH(21)c	2.17	*M*(12)–OH(15)	2.10
M(5)–OH(22)c	2.18	*M*(12)–OH(17)	2.07
<*M*(5)–O>	2.22	<*M*(12)–O>	2.12
M(6)–O(3)a	2.15	*M*(13)–O(7)	2.18
M(6)–O(6)	2.24	*M*(13)–OH(2)a	2.17
M(6)–O(10)	2.32	*M*(13)–OH(10)a	2.10
M(6)–OH(7)	2.22	*M*(13)–OH(17)	2.10
M(6)–OH(20)	2.15	*M*(13)–OH(18)	2.06
M(6)–OH(21)	2.15	*M*(13)–OH(19)a	2.08
<*M*(6)–O>	2.21	<*M*(13)–O>	2.12
M(7)–O(2)	2.14	*M*(14)–OH(2)	1.96
M(7)–O(5)c	2.27	*M*(14)–OH(10)	1.96
M(7)–O(10)	2.33	*M*(14)–OH(11)	1.96
M(7)–OH(6)c	2.24	*M*(14)–OH(12)	1.97
M(7)–OH(20)	2.17	*M*(14)–OH(13)	1.96
M(7)–OH(22)	2.14	*M*(14)–OH(14)c	1.96
<*M*(7)–O>	2.22	<*M*(14)–O>	1.96

all esds. are 0.02

a: $x-\frac{1}{2}, y-\frac{1}{2}, z$; b: $x+1, y, z$; c: $x+\frac{1}{2}, y-\frac{1}{2}, z$; d: $x+\frac{1}{2}, y+\frac{1}{2}, z$; e: $x-\frac{1}{2}, \bar{y}+\frac{1}{2}, z-\frac{1}{2}$; f: $x-\frac{1}{2}, y+\frac{1}{2}, z$; g: $x-1, y, z$.

TABLE 4. SITE OCCUPANCIES FOR ARAKIITE

	As^{5+}	As^{3+}	Fe^{3+}	Al^{3+}	Zn	Mn^{2+}	Mg
As(1)	1.00						
As(2)		1.00					
As(3)	1.00						
T(1)					0.71(7)	0.29(7)	
M(1)						1.00	
M(2)						1.00	
M(3)						1.00	
M(4)			1.00				
M(5)						1.00	
M(6)						1.00	
M(7)						1.00	
M(8)						0.80(4)	0.20(4)
M(9)						0.10(4)	0.90(4)
M(10)						0.13(4)	0.87(4)
M(11)						0.31(4)	0.69(4)
M(12)						0.28(4)	0.72(4)
M(13)						0.15(4)	0.85(4)
M(14)			0.26(3)	0.74(3)			

TABLE 5. CHEMICAL COMPOSITION (wt.%) AND *UNIT FORMULA (*apfu*) OF ARAKIITE

As_2O_5	15.84(38)	As^{5+}	2.08
**As_2O_3	6.56(38)		
ZnO	4.48(17)	As^{3+}	1
MnO	34.32(34)		
MgO	12.76(34)	Zn	0.83
Fe_2O_3	6.76(27)	Mn^{2+}	0.17
Al_2O_3	2.25(14)	Σ	1
†H_2O	-13.74		
	96.71	Mn^{2+}	6
		Mg	4.77
		Mn^{2+}	1.12
		Σ	5.89
		Fe^{3+}	1.28
		Al	0.67
		Σ	1.95
		OH	(23)

Not detected: Na, Ca, K, Ti, V, Cr, Cu, Si, P, S, F.

*based on 34 oxygen atoms;
** based on 1 As^{3+} *apfu*;
†based on 23 (OH) *apfu*.

constituent cations were identified by site-occupancy refinement (Table 4), the unit formula as derived from the chemical composition (Table 5), and the local stereochemistry about each site (Table 3).

The As sites

Three sites have X-ray scattering powers of ~33 e^-; these are labeled *As* and are occupied by As. The *As*(1) and *As*(3) sites are each coordinated by a tetrahedral arrangement of four O atoms, with <*As*–O> distances of 1.71 and 1.69 Å, respectively; the *As*–O distances are in the range 1.68–1.74 Å. All these values are typical for pentavalent As, and hence the *As*(1) and *As*(3) sites are occupied by As^{5+}. The *As*(2) site is coordinated by three O atoms arranged in a triangle displaced to one side of the *As*(2) site such that the $As(2)O_3$ polyhedron is a triangular pyramid; the <As(2)–O> distance is 1.77 Å, and the *As*(2)–O distances are in the range 1.76–1.78 Å. This stereochemistry is typical of As^{3+} with a stereoactive lone pair of electrons; thus the *As*(2) site is occupied by As^{3+}.

The T site

There is one site coordinated by four O atoms in a tetrahedral arrangement with a <*T*(1)–O> distance of 1.99 Å and *T*(1)–O distances in the range 1.97–2.00 Å. The chemical composition derived from electron-microprobe analysis (Table 5) and the refined site-scattering value indicate that the *T*(1) site must be occupied primarily by Zn, as the refined site-scattering at the *T*(1) site (~29 e^-) significantly exceeds all other possible scatterers for this site. The <*T*(1)–O> distance indicates occupancy by a second cation that must be larger than Zn. The chemical composition indicated that this second cation could be Fe^{2+} or Mn^{2+}. However, as we will show later, all Fe is distributed over the *M*(4) and *M*(14) sites as Fe^{3+}, leaving Mn^{2+} to occupy *T*(1). At the final stages of refinement, the site occupancy was refined in terms of Zn and Mn (Table 4). Although Mn^{2+} is unusual in tetrahedral coordination, there are minerals in which this does occur. For example, akatoreite, $Mn^{2+}_9Al_2Si_8O_{24}(OH)_8$ (Burns & Hawthorne 1993) and philolithite (Kampf *et al.* 1998) have Mn^{2+} in both octahedral and tetrahedral coordinations.

The M sites

There are fourteen crystallographically distinct *M* sites, each of which is surrounded by six anions in an octahedral arrangement. Site-scattering refinement and the restrictions imposed by the unit formula of arakiite (Table 5) indicate that seven of the *M* sites are occupied solely by Mn or Fe (or both): *M*(1) to *M*(7). The <*M*(4)–O> distance is 2.03 Å, and the other <*M*–O> distances in the range are 2.19–2.22 Å. The latter distances are compatible with the occupancy of the *M*(1), *M*(2), *M*(3), *M*(5), *M*(6) and *M*(7) sites by Mn^{2+}: 0.83 + 1.36 = 2.19 Å, radii from Shannon (1976). The <*M*(4)–O> distance of 2.03 Å is compatible with occupancy of the *M*(4) site by Mn^{3+} or Fe^{3+}: 0.645 + 1.35 = 2.00 Å, radii from Shannon (1976). The Mn^{3+} cation has a d^4 electron configuration and shows Jahn–Teller distortion where in octahedral coordination (Burns *et al.* 1994); typically, this phenomenon results in four short Mn^{3+}–O distances (~1.95 Å) and two long Mn^{3+}–O distances (~2.28 Å). The *M*(4)–O distances in arakiite show little deviation from the <*M*(4)–O> distance of 2.03 Å, compatible with

occupancy of the $M(4)$ site by Fe^{3+} and *not* by Mn^{3+}.

The $<M(14)–O>$ distance is 1.96 Å. Inspection of the cations available to assign to this site (Table 5), together with the refined site-scattering value, indicates that the $M(14)$ site must be occupied by Al and Fe^{3+} or Mn^{3+}; the small dispersion of $M(14)$–O distances indicates that this site is occupied by Al and Fe^{3+} rather than Mn^{3+}. This assignment of valence states is in accord with that observed in the related minerals hematolite, dixenite and "ferric-hematolite", all of which occur at Långban.

The $M(8)$–$M(13)$ sites have refined site-scattering values indicating occupancy by (Mg,Al) and (Mn,Fe). However, all Al and Fe has already been assigned to the $M(4)$ and $M(14)$ sites, and hence the $M(8)$–$M(13)$ sites are occupied by Mg and Mn. The $<M–O>$ distances for the $M(8)$–$M(13)$ are compatible with occupancy of these sites by Mg and Mn^{2+}.

In the final stages of refinement, the site-scattering factors were assigned as indicated above, and site occupancies were refined together with all other variables. The final site-occupancies are given in Table 4.

Mean bond-lengths

The mean bond-lengths as a function of constituent-cation radius are shown in Figure 1; the line in Figure 1 is a least-squares fit to the arakiite data. The linear fit and the slope of ~1.0 indicate agreement with a simple hard-sphere model of empirical radii, and support the site occupancies assigned in Table 4. The data for hematolite, taken from Moore & Araki (1978), are also shown as unshaded circles in Figure 1; these data fit the trend for the arakiite data, supporting the site assignments in both structures. The cation assignments for the $M(5)$ and $M(7)$ sites in hematolite (Moore & Araki 1978) have been altered from $M(5)$ = 0.44 Al + 0.40 Mg + 0.16 Mn^{2+} and $M(7)$ = 0.58 Al + 0.19 Fe^{3+} + 0.23 Mn^{2+} to $M(5)$ = 0.42 Al + 0.42 Mg + 0.16 Mn^{2+} and $M(7)$ = 0.58 Al to 0.16 Fe^{3+} + 0.26 Mn^{2+} to yield overall electroneutrality.

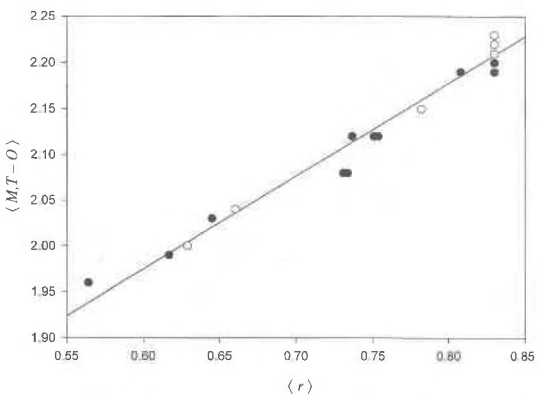

FIG. 1. Variation in mean bond-length with aggregate constituent ionic-radius for the M and T sites in arakiite (shaded circles) and hematolite (unshaded circles); note that several data-points overlap, and that the site occupancies for $M(5)$ and $M(7)$ in hematolite have been slightly modified (see text) to produce electroneutrality.

There is an apparent discrepancy between the refined occupancies (Table 4) and the chemical composition (Table 5) for all multiple-component sites [$T(1)$, $M(8)$ → $M(14)$] in arakiite. The crystal used for structure refinement is slightly deficient in Zn and slightly enriched in Al relative to the crystal used for electron-microprobe analysis. The refined crystal contains ~4.2 Mg *pfu* and ~8.1 Mn^{2+} *pfu* (per formula unit) as compared to ~4.8 Mg and ~7.3 Mn^{2+} for the analyzed crystal. The linear fit between the mean bond-lengths and constituent-cation radius (Fig. 1) supports the site occupancies of Table 4; we conclude that the crystal used for structure refinement is chemically somewhat different than the crystal used for electron-microprobe analysis.

STRUCTURE TOPOLOGY

There are five distinct sheets of polyhedra stacked along the c axis; these sheets are labeled m = 0 to m = 4 according to their relative height along c. Four of these sheets are shown in idealized form in Figure 2; the bold hexagonal cell shown facilitates visual stacking of the four sheets, and is conformable with the unit cell of hematolite (space group $R\bar{3}$). The m = 1 sheet (Fig. 2a) consists of a sheet of edge-sharing octahedra in which 4/7 of the octahedral sites are occupied; vacant octahedra are associated together in a trimer in which each octahedron shares an edge with each of the other octahedra. An (AsO_4) tetrahedron attaches to the inner periphery of each vacancy trimer to produce a sheet of general composition [$\square_3M_4(TO_4)\phi_{10}$]. The m = 2 sheet (Fig. 2b) is a sheet of edge-sharing octahedra in which 3/7 of the octahedral sites are occupied. This sheet is the inverse of the m = 1 sheet: all vacant octahedra in the m = 1 sheet correspond to occupied octahedra in the m = 2 sheet, and all occupied octahedra in the m = 1 sheet correspond to vacant octahedra in the m = 2 sheet. The occupied octahedral trimers in the m = 2 sheet are linked by (AsO_3) groups (Fig. 2b) that overlie the occupied octahedral trimers in the m = 1 sheet, giving a general composition [$\square_4M_3(TO_3)\phi_{10}$]. The m = 3 sheet (Fig. 2c) consists of isolated occupied octahedra and isolated (AsO_4) groups. Each octahedron shares three edges with the underlying trimer of occupied octahedra in the m = 2 layer, and each tetrahedron opposes the non-trimer vacant octahedron in the m = 2 layer. The m = 3 sheet also has an anion vacancy in its lower layer of O atoms (shown by the broken circle in Fig. 2c) that matches with the (AsO_3) group of the m = 2 sheet, providing room for the stereoactive lone-pair of electrons

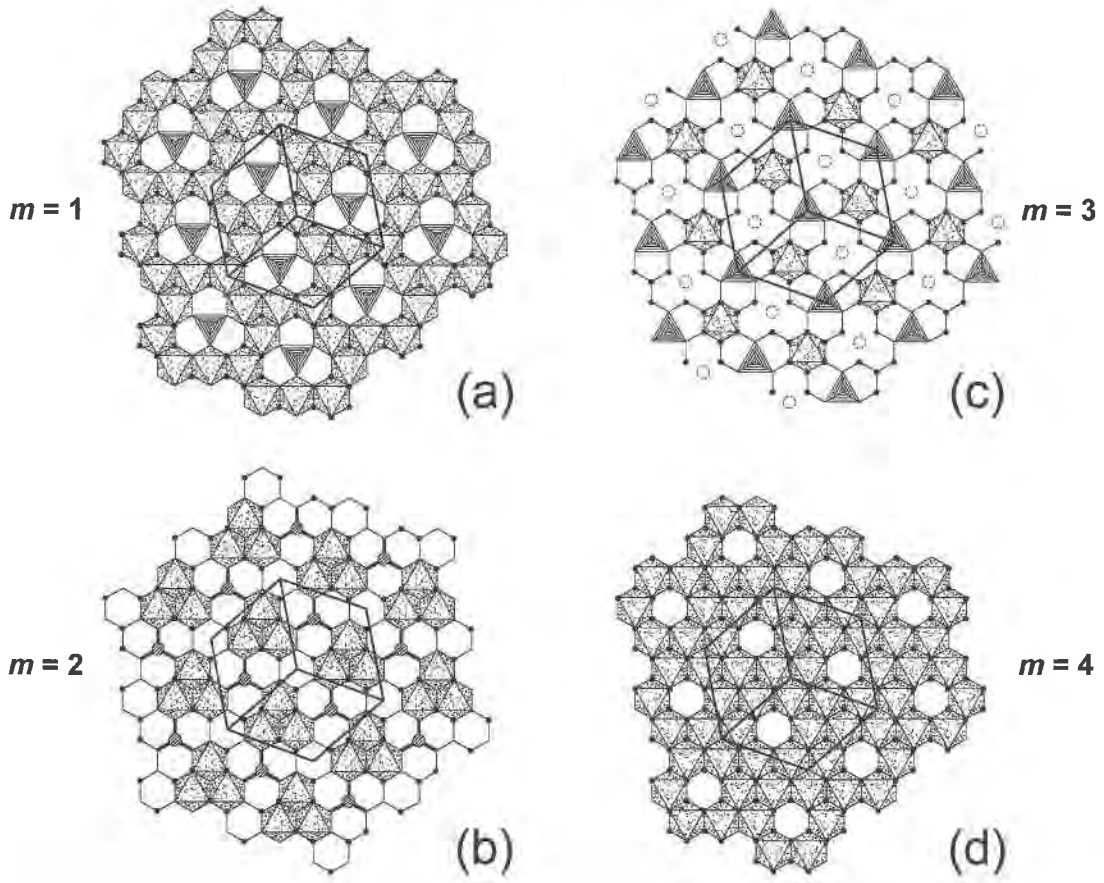

FIG. 2. The polyhedral layers for $m = 1$ to $m = 4$ in arakiite and hematolite: (a) $m = 1$; (b) $m = 2$; (c) $m = 3$; (d) $m = 4$; MO_6 octahedra: random dot-shading; AsO_4 tetrahedra: line-shading; As^{3+} cations: large diagonal-line-shaded circles; As^{3+}–O bonds: thick lines; small shaded circles: (OH) groups; broken circles: anion vacancies.

of the As^{3+} cation, resulting in the general composition $[\square_6 M_1(TO_4)\phi_9]$. The $m = 4$ sheet (Fig. 2d) is a sheet of edge-sharing octahedra with isolated vacancies, and has the general composition $[\square M_6\phi_{14}]$. The $m = 0$ layer (not shown in Fig. 2) consists of isolated $T(1)$ tetrahedra; it has the general composition $[\square_7(T\phi_4)\phi_{10}]$.

Relation to Hematolite

The structure of arakiite, $^{[4]}(Zn,Mn^{2+})$ $(Mn^{2+},Mg)_{12}$ $(Fe^{3+},Al)_2$ $(As^{3+}O_3)$ $(As^{5+}O_4)_2$ $(OH)_{23}$, is very similar to that of hematolite: $^{[6]}(Mn^{2+})$ $(Mn^{2+},Mg)_{12}$ $(Al,Fe^{3+})_2$ $(As^{3+}O_3)$ $(As^{5+}O_4)_2$ $(OH)_{23}$ (Moore & Araki 1978). Both structures contain close-packed layers of anions with five crystallographically distinct sheets of polyhedra constituting the asymmetric unit. The four sheets shown in Figure 2 occur in both arakiite and hematolite, the topologies being identical (although the chemical compositions differ somewhat). Their stacking sequences are shown in Figure 3. Arakiite is a close-packed packet structure with five layers of O atoms that stack along the c axis according to the sequence $\cdot$ $^{**}hch$ $\cdot$ (where c corresponds to cubic close-packing; h to hexagonal close-packing, and * denotes an anion layer that is not close-packed). The anion stacking-sequence in arakiite differs from that in hematolite, $\cdot$ $hhhch$ $\cdot$. The resulting differences in the $m = 0$ sheets and meshing of the $m = 4$, 0 and 1 sheets are shown in Figure 4. The topology, but not the cation order, in the $m = 4$ sheets is the same in both structures, and the anions of this sheet that coordinate the $m = 0$ cations are topologically identical in both structures. However, the difference in anion packing in the anion layers on either side of the $m = 0$ sheet (** in arakiite and hh in hematolite) result in tetrahedrally coordinated cations in the $m = 0$ sheet of arakiite (Fig. 4a) and octahedrally coordinated cations in the $m = 0$ sheet

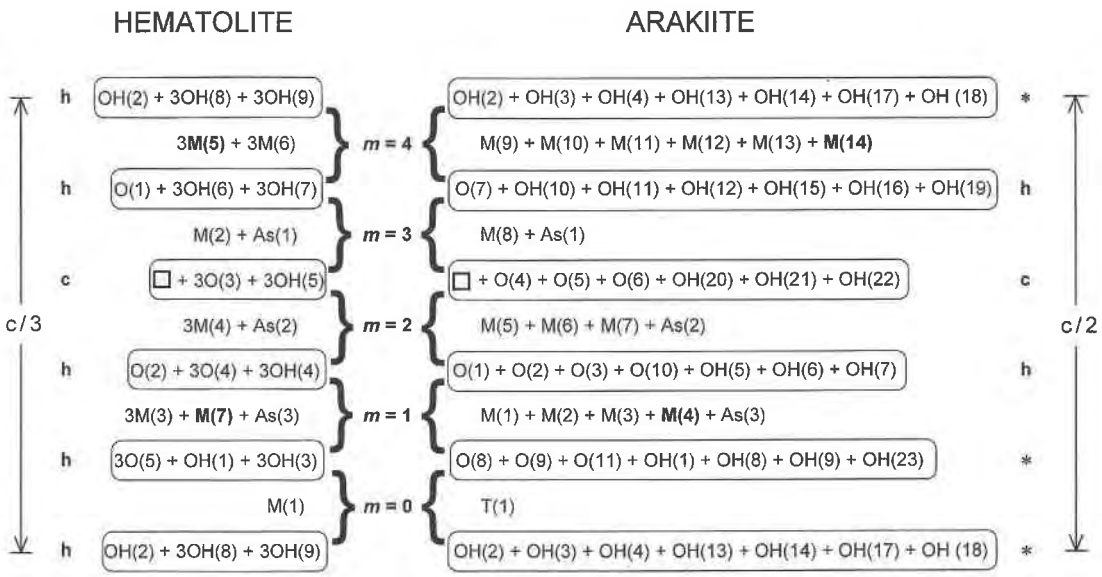

FIG. 3. The sheet-stacking sequences in hematolite (left) and arakiite (right). The various anion layers are shown in round-cornered boxes, together with the type of anion packing (*c*: cubic close-packed, *h*: hexagonal close-packed, *: non-close-packed) at the left and right margins of the figure. The cations of the sheets are shown intercalated between the anion layers with the sheet numbering ($m = 0$ to $m = 4$) shown in heavy symbols at the center of the diagram. The cation sites denoted in bold contain octahedrally coordinated trivalent cations (Fe^{3+} and Al); coefficients denote number of sites *pfu*.

of hematolite (Fig. 4b); it is this $m = 0$ sheet that is the principal difference between the two structures. As shown in Figure 5a, the anion layers on either side of the $m = 0$ layer in hematolite are close-packed, whereas the analogous anions layers in arakiite show significant deviation from close-packing (Fig. 5b). This difference is most easily visualized by focusing on the (white) holes between the anions in Figure 5; in Figure 5a, the holes occur at the vertices of a 3^6 net, whereas in Figure 5b, the holes have coalesced to form sinuous broken channels. Whereas the anions forming the ligands of the *T*(1) tetrahedron are locally close-packed in arakiite, the remaining anions are significantly displaced from their ideal close-packed positions. Thus it is better to describe the packing in arakiite by the symbol !***hch*! where the star denotes a non-close-packed layer, and refer to it as a *packet* structure as it consists of packets of close-packed anion layers, rather than a continuous close-packed arrangement of layers. The linkage between the $m = 0$ and $m = 1$ sheets is also shown in Figure 4. In arakiite, the single apical vertex of a tetrahedron links to the lower anion of an edge shared between two octahedra (Fig. 4a), whereas in hematolite, the upper three vertices of the octahedron link to the lower three vertices of an octahedron [*M*(7)] in the $m = 1$ sheet, producing face-sharing of octahedra. The $m = 1$ sheets in arakiite and hematolite are enantiomers (Figs. 4a, b), and in arakiite, the sheets separated by *c*/2 also are enantiomers.

The unit-cell relations between the two structures are shown in Figure 5 and Table 6. In the plane of the cation sheets, hematolite has hexagonal cell-dimensions of 8.275 Å, which we can write as a_H. The cell dimensions of arakiite are those of the *C*-centered-equivalent cell with $a_A = \sqrt{3}\ a_H$ and $b_A = a_H$. As noted by Moore & Araki (1978), the close-packed nature of the hematolite structure allows interpretation of the *c* dimension in terms of a multiple of the thickness of a close-packed sheet: 2.4 Å. Thus $c_H \approx 2.4 \times 15$ Å and $c_A \approx 2.4 \times 10$ Å. The stacking sequence in hematolite produces α and γ angles of 90°, resulting in a hexagonal (rhombohedral) cell. This is not the case in arakiite; the non-close-packed anion layers (**) on either side of $z = 0$ contain a displacement in the *a*–*b* plane relative to the arrangement in hematolite, producing the monoclinic unit-cell.

TABLE 6. CELL DIMENSIONS OF HEMATOLITE AND ARAKIITE

	Hematolite	Arakiite
a (Å)	8.275 = a_H	14.236 ~ $\sqrt{3}\ a_H$
b	= *a* = a_H	8.206 ~ a_H
c	36.60 ~ 2.4 x 15	24.225 ~ 2.4 x 10
β (°)	90	93.52

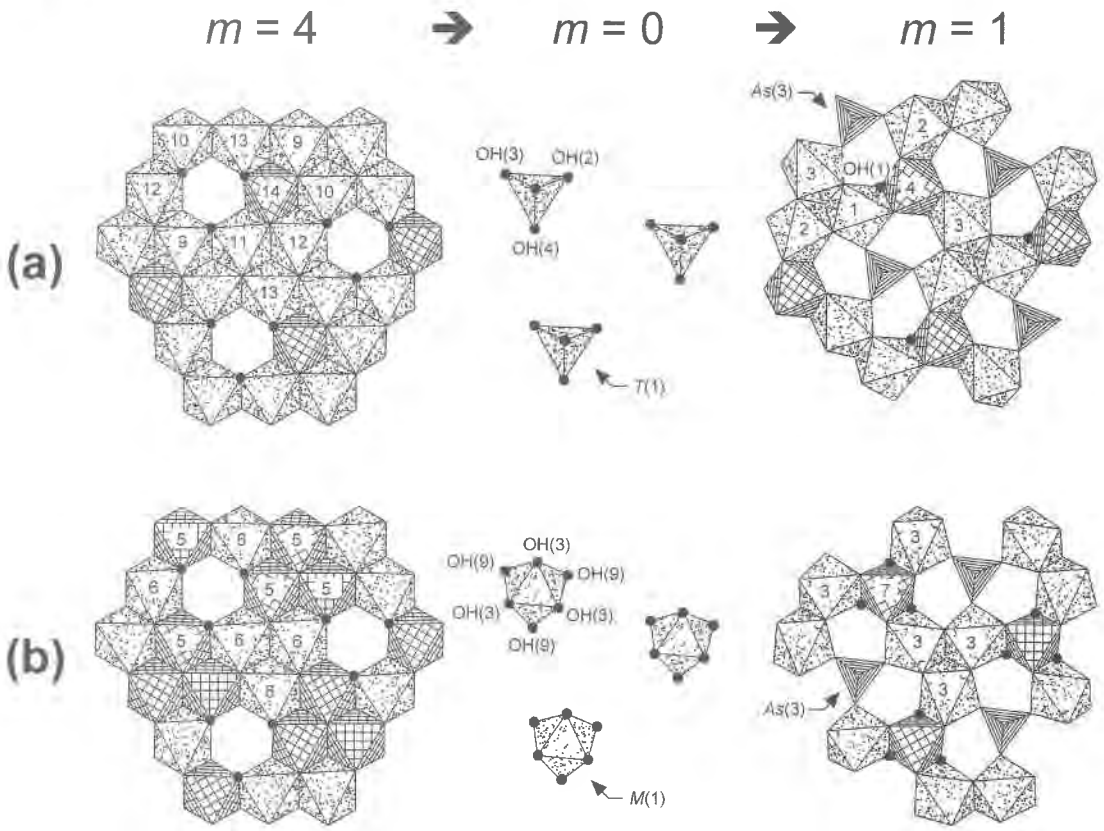

FIG. 4. The linkage between the $m = 4$, 0 and 1 sheets in (a) arakiite, and (b) hematolite, projected onto (001). Octahedra that are random dot-shaded contain divalent cations; in arakiite, octahedra with 4^4 shading contain trivalent cations; in hematolite, octahedra with 4^4 shading contain both trivalent and divalent cations; line-shaded tetrahedra are $(As^{5+}O_4)$ groups; random-dot-shaded tetrahedra [involving the $T(1)$ sites in arakiite] contain divalent cations; the black-shaded circles are (OH) groups involved in linking the $m = 4$ layer to the $m = 1$ layer through the $m = 0$ layer; the numbers on the octahedra show that they are M octahedra involving the M site designated by the number itself

CATION ORDER IN ARAKIITE AND HEMATOLITE

The cation distribution (in *apfu*) in the five unique sheets of hematolite and arakiite is shown in Figure 6. The anion compositions at the sheet boundaries are identical in the two structures; the anion component differs only in the relative stacking across the $m = 0$ sheet. The aggregate cation-charge (45$^+$ *pfu*) must therefore be equal in both structures. The $(As^{3+}O_3)(As^{5+}O_4)_2(OH)_{23}$ component of these two structures is invariant (32$^-$ *pfu*), and the overall ratio $M^{3+}/(M^{2+} + M^{3+})$ of the remaining cations is fixed at 2/15 *apfu* (32$^+$ *pfu*). This holds true for all chemical compositions of hematolite and "ferric-hematolite" (Dunn & Peacor 1983).

Intersheet order

Comparison of the cation charges at the left and right edges of Figure 6 shows that the only differences in charge distribution occur on either side of the $m = 0$ sheet. The M^{3+} cations in hematolite exceed 1 *apfu* in the $m = 4$ sheet, and show a complementary deficiency in the $m = 1$ sheet, whereas arakiite contains one M^{3+} cation in both the $m = 1$ and $m = 4$ sheets.

The principal difference between the two structures occurs in the $m = 0$ sheet: Mn^{2+} is octahedrally coordinated by 6 (OH) groups in hematolite, and (Zn,Mn^{2+}) is tetrahedrally coordinated by 4 (OH) groups in arakiite. The cation charge in the $m = 0$ sheet is identical (2$^+$ *pfu*) in the two structures, and so is the nature of the bordering anions. Is the difference in cation coordination (octahedral *versus* tetrahedral) in the $m = 0$ sheet related to the different M^{2+}–M^{3+} distributions in the adjoining $m = 1$ and $m = 4$ sheets? The cation coordinations for the $m = 0$ sheets are shown in Figure 7, the $M(1)$ octahedron in hematolite (Fig. 7a) and the $T(1)$ tetrahedron in arakiite (Fig. 7b); the associated Pauling bond-strengths appear as labels adjacent to the bonds in Figure 7. The

TABLE 7. BOND-VALENCE TABLE FOR ARAKIITE

	T(1)	*As*(1)	*As*(2)	*As*(3)	*M*(1)	*M*(2)	*M*(3)	*M*(4)	*M*(5)	*M*(6)	*M*(7)	*M*(8)	*M*(9)	*M*(10)	*M*(11)	*M*(12)	*M*(13)	*M*(14)	
O(1)			0.98		0.24		0.31		0.40										1.93
O(2)			0.98			0.31	0.25				0.38								1.92
O(3)			1.02		0.33	0.25				0.37									1.97
O(4)		1.25							0.25										1.50
O(5)		1.19									0.27								1.46
O(6)		1.19								0.29									1.48
O(7)		1.08													0.27	0.29	0.29		1.93
O(8)				1.25	0.41														1.66
O(9)				1.22		0.44													1.66
O(10)				1.22					0.23	0.24	0.23								1.92
O(11)				1.19			0.41												1.60
OH(1)	0.47				0.31			0.47											1.25
OH(2)	0.52																0.30	0.48	1.30
OH(3)	0.47													0.36		0.37			1.20
OH(4)	0.50												0.36		0.35				1.21
OH(5)						0.32		0.41	0.31										1.04
OH(6)					0.33			0.46			0.29								1.08
OH(7)							0.32	0.47		0.31									1.10
OH(8)							0.34	0.56											0.90
OH(9)						0.35		0.47											0.82
OH(10)													0.33				0.34	0.48	1.15
OH(11)														0.33		0.34		0.48	1.15
OH(12)												0.31			0.33			0.47	1.11
OH(13)													0.32	0.30				0.48	1.10
OH(14)															0.36	0.32		0.48	1.16
OH(15)												0.35	0.37			0.36			1.08
OH(16)													0.39	0.38	0.37				1.14
OH(17)													0.37			0.38	0.34		1.09
OH(18)														0.39	0.37		0.37		1.13
OH(19)												0.37		0.38			0.36		1.11
OH(20)										0.37	0.35	0.32							1.04
OH(21)									0.35	0.37		0.31							1.03
OH(22)									0.34		0.38	0.28							1.00
OH(23)					0.37	0.33	0.35												1.05
	1.96	4.71	2.98	4.88	1.99	2.00	1.98	2.84	1.88	1.95	1.90	1.94	2.14	2.14	2.05	2.06	2.00	2.87	

anions bordering the overlying $m = 1$ sheet receive a greater bond-strength contribution from the $m = 0$ sheet cations in hematolite (1.0 valence unit, *vu*) and a lesser contribution (0.5 *vu*) in arakiite, per cation. The anions bordering the underlying $m = 4$ sheet receive a greater relative bond-strength contribution in arakiite (1.5 *vu*) and a lesser contribution (1.0 *vu*) in hematolite.

The relative increase in cation charge (Fig. 6) in the $m = 1$ sheet of arakiite (14^+ as compared to 13.75^+ in hematolite) and the relative decrease in cation charge in the $m = 4$ sheet of arakiite (13^+ as compared to 13.25^+ in hematolite) serve to stabilize the bond-strength requirements of the anions of the $m = 0$ sheet, resulting from occupation of the $m = 0$ sheet in arakiite by tetrahedra. Thus incorporation of the $^{[4]}(Zn,Mn^{2+})$ cations in the $m = 0$ sheet of arakiite drives a $M^{3+} \rightarrow M^{2+}$ substitution in the overlying $m = 1$ sheet and a $M^{2+} \rightarrow M^{3+}$ substitution in the underlying $m = 4$ sheet, relative to the cation distribution in the comparable sheets in hematolite.

Cation order involving the m = 4 sheet: In the previous section, we saw that occupancy of the $m = 0$ sheet in hematolite by octahedrally coordinated Mn^{2+} cations coincides with an excess of one M^{3+} cation in the $m = 4$ sheet. This M^{3+} content occurs in hematolite as (1.26 Al + 0.48 Mn^{2+} + 1.26 Mg) *pfu* disordered over three equivalent *M*(5) sites (Fig. 4b). The triplet of *M*(5) sites in hematolite (Fig. 4b) correlates with the *M*(9), *M*(10) and *M*(14) sites in arakiite (Fig. 4a). The lower (monoclinic) symmetry of arakiite allows ordering over these analogous sites; thus the *M*(9) and *M*(10) sites are occupied solely by divalent cations ($Mg > Mn^{2+}$), whereas the *M*(14) site is occupied entirely by trivalent cations ($Al > Fe^{3+}$) (Table 4). The remaining triplet of symmetrically equivalent *M*(6) sites in hematolite (Fig. 4b) contains (1.68 Mn^{2+} + 1.32 Mg) *pfu*. The corresponding triplet in arakiite [*M*(11), *M*(12), and *M*(13)] (Fig. 4a) contains ($Mg > Mn^{2+}$) (Table 4).

Why does Fe^{3+} disorder over the *M*(5) triplet and not the *M*(6) triplet in hematolite? Comparison of Figures 2c, 2d shows that the apical oxygen [O(1)] of the (AsO_4) group is shared among the triplet of *M*(6) octahedra. Ordering of M^{3+} at *M*(6) would result in an excess of incident bond-strength at O(1) [5/4 + 1/3 + 1/3 + 1/2 = 2.42 *vu*]. The OH(2) group is shared among the triplet

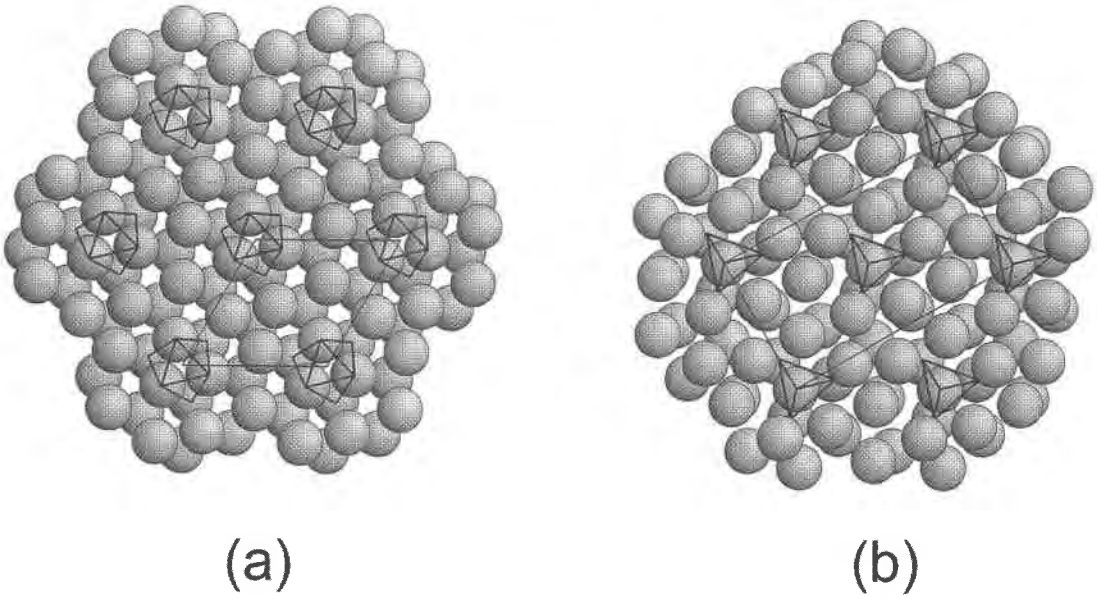

FIG. 5. The anion layers on either side of the $m = 0$ sheet in (a) hematolite and (b) arakiite, projected onto (001). The $M(1)$ octahedra in hematolite and the $T(1)$ tetrahedra in arakiite are outlined; the cell outlines show the hexagonal P-cell for (a) hematolite, and the related monoclinic C-cell for (b) arakiite.

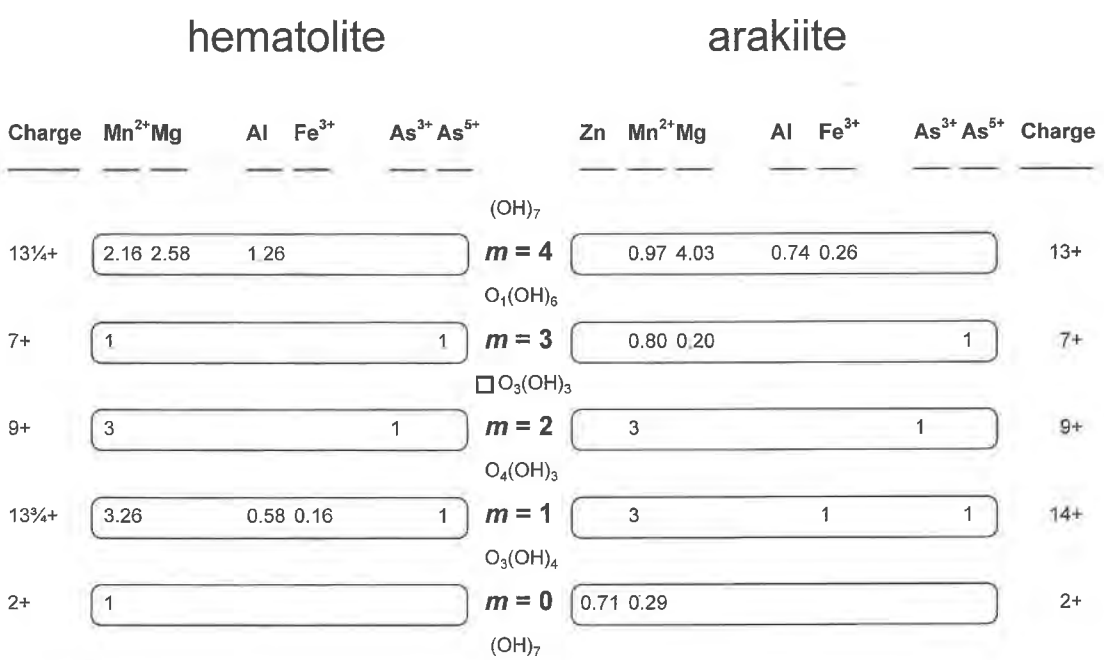

FIG. 6. The cation distribution in hematolite (left) and arakiite (right) over the five unique sheets is shown enclosed in round-cornered boxes (*apfu*) The aggregate-cation charge for each sheet is shown at the left or right margin of the figure.

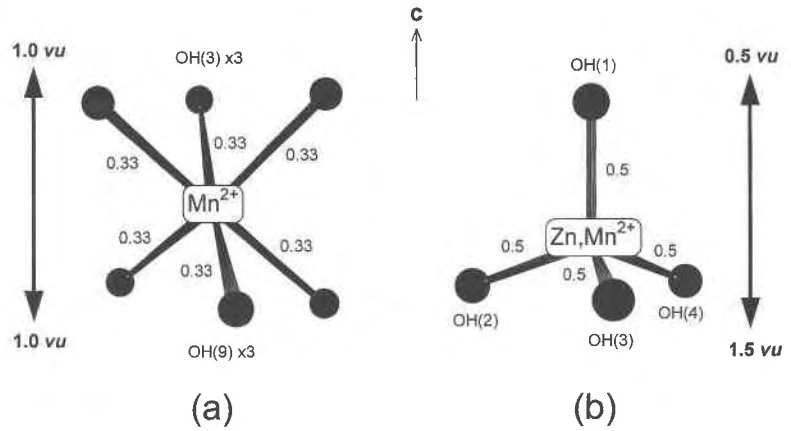

FIG. 7. The cation coordinations for the $m = 0$ sheet in (a) hematolite, and (b) arakiite, with [001] up the page. Numerical labels adjacent to bonds are Pauling bond-strengths. The arrows at the left and right margins show the bond-strength distributions directed above and below the $m = 0$ cations.

of $M(5)$ cations and does not bond to the overlying $M(1)$ octahedron of the $m = 0$ sheet. Thus M^{3+} is able to disorder over the $M(5)$ sites and thereby help satisfy the bond-strength requirements of OH(2) [1/3 + 1/3 + 1/2 = 1.17 *vu*].

For the same reason, we would not expect the (Al,Fe^{3+}) cations in arakiite to occupy the $M(11)$, $M(12)$, or $M(13)$ sites, but why do these trivalent cations order onto $M(14)$ and not $M(9)$ or $M(10)$? There is no obvious crystal-chemical reason for this behavior; we can only speculate that local Mg–Mn^{2+} order over the neighboring octahedral sites and Zn–Mn^{2+} order at the $T(1)$ site are somehow tied to the occurrence of only trivalent cations at $M(14)$. One could also postulate that a modified H-bonding scheme may occur in this region of the structure as a result of tetrahedral coordination of cations in the $m = 0$ sheet.

Cation order involving the m = 3 sheet: Another difference between the two minerals with respect to Mg and Mn^{2+} content occurs at the single octahedron of the $m = 3$ sheet. The $M(2)$ octahedron in hematolite contains only Mn^{2+}, whereas the analogous $M(8)$ octahedron in arakiite contains appreciable Mg (Figs. 3, 6). Comparison of Figures 2c and 2d shows that these isolated octahedra of the $m = 3$ sheet share the three lower vertices of the octahedral hole in the $m = 4$ sheet. Local order of Al–Fe^{3+} at $M(14)$ could be influenced by local order of (Mn^{2+}–Mg) at $M(2)$ in arakiite, as the occupancy ratios are comparable.

Cation order involving the m = 2 sheet: The cation arrangement in the $m = 2$ sheet is identical in both structures.

Cation order involving the m = 1 sheet: The trivalent cations in the $m = 1$ sheet of hematolite occur as (0.58 Al + 0.16 Fe^{3+} + 0.26 Mn^{2+}) *pfu* occupying the $M(7)$ site (Figs. 3, 6). In arakiite, the $M(4)$ site is fully occupied by Fe^{3+}. In both structures, the adjoining trimer of octahedra [hematolite: $M(3) \times 3$; arakiite: $M(1)$, $M(2)$, $M(3)$] contains only Mn^{2+} cations. Why do the trivalent cations in both structures reside in a single octahedron at the juncture of the three surrounding octahedral triplets? Examination of Figures 2a and 2b shows that the As^{3+} cation sits over the center of the octahedral triplet. Each of the O^{2-} anions at the center of the triplet bonds to As^{3+} ($m = 2$), Mn^{2+} ($m = 2$), and two Mn^{2+} ($m = 1$). The incident bond-strength sum at these anions is (3/3 + 1/3 + 1/3 + 1/3 = 2 *vu*), and their bond-strength requirements are satisfied; hence, trivalent cations do not occupy the triplet of octahedra.

A special condition exists in the $m = 1$ sheet of arakiite as a result of the occupancy of the tetrahedra in the underlying $m = 0$ sheet. The OH(1) anion bonds to $M(1)$, $M(4)$ and $T(1)$ (Fig. 4); however, the other lower two anions of the $M(4)$ octahedron [OH(8) and OH(9)] are coordinated only by $M(4)$ and either $M(2)$ or $M(3)$. The bond-strength sums of these [2]-coordinated anions, OH(8) and OH(9), are only 0.90 and 0.82 *vu*, respectively [Table 7; calculated from the parameters of Brown (1981)]. Each of these anions will also require an additional H-bond in order to satisfy their incident bond-strength requirements. This condition at OH(8) and OH(9) requires that $M(4)$ be occupied only by trivalent cations.

ACKNOWLEDGEMENTS

We thank Dr. Mark Feinglos for use of his material in this work, and Paulus B. Moore and a pseudo-anony-

mous referee for their comments on this paper; Paulus suggested use of the term "packet structure". Financial support was provided by Natural Sciences and Engineering Research Council (of Canada) grants to FCH.

References

BROWN, I.D. (1981): The bond-valence method: an empirical approach to chemical structure and bonding. *In* Structure and Bonding in Crystals II (M. O'Keeffe and A. Navrotsky, eds.). Academic Press, New York, N.Y (1-30).

BURNS, P.C., COOPER, M.A. & HAWTHORNE, F.C. (1994): Jahn–Teller-distorted $Mn^{3+}O_6$ octahedra in fredrikssonite, the fourth polymorph of $Mg_2Mn^{3+}(BO_3)O_2$. *Can. Mineral.* **32**, 397-403.

_____ & HAWTHORNE, F.C. (1993): Edge-sharing $Mn^{2+}O_4$ tetrahedra in the structure of akatoreite, $Mn^{2+}{}_9Al_2Si_8O_{24}(OH)_8$. *Can. Mineral.* **31**, 321-329.

DUNN, P.J. & PEACOR, D.R. (1983): A ferric ion equivalent of hematolite from Sterling Hill, New Jersey and Långban, Sweden. *Mineral. Mag.* **47**, 381-385.

IBERS, J.A. & HAMILTON, W.C., eds. (1974): *International Tables for X-ray Crystallography* IV. Kynoch Press, Birmingham, U.K.

KAMPF, A.R., MOORE, P.B., JONSSON, E.J. & SWIHART, G.H. (1998): Philolithite, a new mineral from Långban, Värmland, Sweden. *Mineral. Rec.* **29**, 201-206.

MOORE, P.B. & ARAKI, T. (1978): Hematolite: a complex dense-packed sheet structure. *Am. Mineral.* **63**, 150-159.

POUCHOU, J.L. & PICHOIR, F. (1985): "PAP" $\phi(\rho z)$ procedure for improved quantitative microanalysis. *In* Microbeam Analysis (J.T. Armstrong, ed.). San Francisco Press, San Francisco, California (104-106).

ROBERTS, A.C., COOPER, M.A., HAWTHORNE, F.C., GRICE, J.D. & FEINGLOS, M.N. (2000): Arakiite, a new Zn-bearing hematolite-like mineral from Långban, Sweden. *Mineral. Rec.* (in press).

SHANNON, R.D. (1976): Revised effective ionic radii and systematic studies of interatomic distances in halides and chalcogenides. *Acta Crystallogr.* **A32**, 751-767.

Received May 27, 1999, revised anuscript accepted December 2, 1999.